Journal of Alloys and Compounds 630 (2015) 172–177

Contents lists available at ScienceDirect

Journal of Alloys and Compounds

journal homepage: www.elsevier.com/locate/jalcom

Microstructures and mechanical properties of friction stir welded lap joints of commercially pure titanium and 304 stainless steel

K. Ishida [a,*], Y. Gao [a], K. Nagatsuka [b], M. Takahashi [b], K. Nakata [b]

[a] Graduate School of Engineering, Osaka University, 11-1 Mihogaoka, Ibaraki 567-0047, Japan
[b] Joining and Welding Research Institute, Osaka University, 11-1 Mihogaoka, Ibaraki 567-0047, Japan

ARTICLE INFO

Article history:
Received 2 October 2014
Received in revised form 3 December 2014
Accepted 2 January 2015
Available online 9 January 2015

Keywords:
Friction stir welding
Dissimilar joint
Mechanical properties
Microstructure
TEM

ABSTRACT

Friction stir welding was performed to accomplish dissimilar lap joining of commercially pure titanium (CP-Ti) to 304 stainless steel (SUS304). The joining speed was varied from 25 to 100 mm min^{-1}. At a joining speed of 50 mm min^{-1}, the morphology of the interface was a flat and simple interfacial reaction layer whose thickness was less than 1 μm. The reaction layer consisted of four layers: β-Ti (+ ω-Ti), Ti_2Ni, FeTi + Fe_2Ti, and σ-FeCr, listed in order from the CP-Ti side to the SUS304 side. At a joining speed of 25 mm min^{-1}, the interface consisted of a macroscopically mixed and laminated structure approximately 300 μm thick consisting of multiple reaction layers. During the tensile shear test, joint fractures occurred in the CP-Ti base material at every joining speed. However, during the peel test, joint fractures occurred at the joint interface.

1. Introduction

Ti alloys are used as construction materials in the power generation and chemical industries; however, wider use of these materials has been limited by their high cost. One solution is to minimize the amount of Ti alloy used by joining the Ti alloy structure to conventional structural steel. However, it is difficult to weld Ti alloys to steel owing to the formation of brittle intermetallic phases such as FeTi and Fe_2Ti [1]. These highly brittle intermetallic phases cause spontaneous cracking in conventional fusion-welded joints. In addition, the mismatch of thermal expansion coefficient between titanium alloys and steel results in significant residual stress in the joint.

There have been a few works on the dissimilar joining of titanium alloys to steel in terms of avoiding the formation of brittle Fe–Ti intermetallic compounds in the joints. Diffusion bonding [2,3], explosive welding [4–6] as a solid-state process, and laser welding [7] as a high-energy-beam welding process have been investigated up to now. These methods are effective to some extent in controlling the formation of brittle intermetallic compounds, but application of the first two methods is restricted by joint configurations and application of the third method is restricted by the high cost involved.

Friction stir welding (FSW), which is a solid-state welding process, is effective in reducing the formation of brittle intermetallic phases owing to its low welding temperature. In addition, FSW has several advantages, such as a high operating efficiency and versatility as compared with conventional solid-state welding processes such as diffusion bonding.

Najafabadi et al. [8,9] studied the FSW technique for joining CP-Ti (industrial pure titanium) to 304 austenitic stainless steel, and they achieved certain dissimilar lap joining by adjusting the tool rotation and joining speeds under a protective atmosphere. The maximum failure load of the joint reached 73% that of the CP-Ti base material. On the other hand, Liao et al. [10] studied the microstructure of the FSW lap joint interface between CP-Ti and a structural steel. They revealed that swirling macro- and micro-intermixed zones of Ti and Fe were found along the interface, where tiny Fe–Ti intermetallic particles were mixed with β-Ti.

Although these studies are important, the relationship between the FSW parameters, the microstructure of the CP-Ti/stainless steel lap joint interface, and the joint strength have not yet been discussed systematically. Therefore, this study was carried out to investigate the effect of the FSW joining speed on the joint characteristics, including the interfacial microstructure, and on the tensile shear strength and interface peel strength of CP-Ti/SUS304 lap joints.

2. Experimental procedures

The materials used in this study were CP-Ti and SUS304. The chemical compositions of these materials are listed in Table 1. A CP-Ti plate with dimensions of 200 mm × 85 mm × 1 mm and a SUS304 plate with dimension of 200 mm × 85 mm × 3 mm were degreased by acetone before joining. Fig. 1 shows

* Corresponding author. Tel.: +81 6 6879 8666; fax: +81 6 6879 8689.
E-mail address: k.ishida@jwri.osaka-u.ac.jp (K. Ishida).

http://dx.doi.org/10.1016/j.jallcom.2015.01.004
0925-8388/

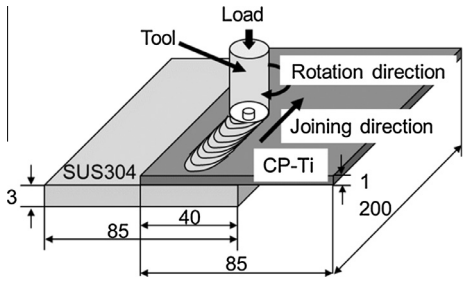

Fig. 1. Schematic illustration of the setup and arrangement of specimens for FSW (in mm).

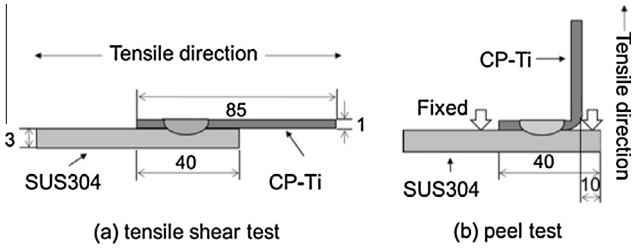

Fig. 2. Schematic illustration of (a) tensile shear test and (b) peel test (in mm).

a schematic illustration of the setup and arrangement of specimens for FSW. The CP-Ti top plate and SUS304 bottom plate were set as a lap joint. FSW was carried out using a WC–Co tool with a 15-mm-diameter shoulder and a 6-mm-diameter pin. The pin length was 1 mm. The tool was tilted at a 3° forward angle from the vertical, and Ar gas was used to prevent surface oxidation during FSW. In terms of the joining parameters, a tool down-force of 9.8 kN was fixed. The tool rotation speeds were varied at 150, 250, 350, and 450 rpm, and the joining speeds were varied at 25, 50, 75, and 100 mm min^{-1}. In order to observe the microstructures of the cross sections of the joints, the joints were cut perpendicular to the joining line and then mechanically polished with abrasive papers and etched with an acid solution of 3 mL HF, 3 mL HNO_3, and 50 mL H_2O. The cross-sectional macrostructures were observed using optical microscopy (OM) and the microstructures were evaluated using scanning electron microscopy (SEM) and electron probe microanalyzer (EPMA). Furthermore, the transmission electron microscopy (TEM) specimens were prepared by focused ion beam (FIB) milling. The interfacial microstructures were assessed using TEM and energy dispersive X-ray spectrometry (EDS) performed at an acceleration voltage of 200 kV. Tensile shear tests and peel tests were carried out to investigate the mechanical properties, as shown in Fig. 2. The joints were cut into strips perpendicular to the joining direction, each with a width of 12 mm, and the strips were tested. Tensile shear tests were performed at room temperature using a precision universal tester operating at a constant crosshead velocity of 1 mm min^{-1} as shown in Fig. 2(a). Peel test specimens were prepared by fixed two point bending of the CP-Ti, followed by dragging at a constant crosshead velocity of 0.5 mm min^{-1} as shown in Fig. 2(b). Three specimens were tested for each joining speed. After the peel test, the fractured surface of the specimen was observed by SEM and EDS.

3. Results and discussion

Fig. 3 shows the combination effect of rotation speed and joining speed on the joint formation in the CP-Ti/SUS304 FSW lap joint. The circles indicate joints with a smooth joint surface and no defects. The squares indicate discontinuous joints with surface defects and burrs; the tool was deformed markedly by joining in these conditions. The X mark indicates a joint that could not be formed because the tool could not be inserted into the CP-Ti plate.

Good joints were formed at rotation speeds of 250 and 350 rpm and at joining speeds from 25 to 100 mm min^{-1}. In contrast, at a rotation speed of 450 rpm, excess heat was generated and the tool was deformed with adhesion of Ti, as shown in Fig. 3d, resulting in a large Ti burr. As a result, the joint was discontinuous. On the other hand, a joint could not be formed at a rotation speed of 150 rpm because less heat was generated to soften the CP-Ti plate, preventing insertion of the tool.

Fig. 4 shows the OM cross sections of joints formed at a constant rotation speed of 250 rpm and joining speeds of 25, 50, and 100 mm min^{-1}. The cross sections with joining speeds of 50 and 100 mm min^{-1} showed flat and smooth interfaces. In contrast, for the joining speed of 25 mm min^{-1}, the joint interface between CP-Ti and SUS304 was unclear. The cross section showed a mixed structure that looked black, as indicated by the dotted circle in Fig. 4. The thickness of the mixed structure was approximately 100–300 μm.

When the joining speed is decreased the plunge depth is increased, besides the tool pin was naturally inserted into the SUS304 side and stirred CP-Ti in with SUS304. Fig. 5 shows a TEM bright-field image (BFI) and the element distributions of Ti, Fe, Ni, and Cr at the interface of the CP-Ti/SUS304 FSW joint formed with a rotation speed of 250 rpm and a joining speed of 50 mm min^{-1}. A reaction layer of uniform thickness formed along the interface, and the total thickness of the reaction layer was approximately 1 μm. The reaction layer was divided into two regions: a diffusion layer and an intermetallic compound layer. Furthermore, the intermetallic compound layer consisted of three different layers: a Ni-rich layer, an Fe-rich layer, and a Cr-rich layer.

Fig. 6 shows a higher magnification TEM micrograph of the rectangular area shown in Fig. 5a. Positions 1–4 from the CP-Ti side were identified as the following phases by selected area electron diffraction (SAD) patterns: Position 1: β-Ti and ω-Ti phases, Position 2: Ti_2Ni phase, Position 3: FeTi and Fe_2Ti phases, and Position 4: σ-FeCr phase. The β-Ti layer at Position 1 is a diffusion layer of Ni and Fe with ω-Ti precipitates [11,12] and Positions 2–4 are intermetallic compound layers.

It has been reported that the maximum temperature at the interface of CP-Ti and SUS304 is beyond 1350 K during FSW [8]. The transformation of β-Ti occurs during FSW at 1155 K. In addition, the transformation temperature of β-Ti decreases with increasing Fe content, and the eutectoid reaction between α-Ti and FeTi occurs at 855 K [1]. Since the cooling rate at the stir zone and particularly at the interfacial zone of dissimilar joints is tremendously high [13], non-equilibrium phases are easily generated in FSW joints [14]. As a result, the β-Ti phase was still present at room temperature and ω-Ti precipitates formed in the β-Ti phase during cooling. In addition, Fe and Ni, which diffuse into β-Ti from SUS304 at elevated temperatures during FSW and are contained in the β-Ti phase, contribute to the stability of the β-Ti phase at temperatures below the eutectoid temperature of 855 K.

The formation of intermetallic compounds of FeTi, Fe_2Ti, and Ti_2Ni is expected, as shown in the binary phase diagrams of the Ti–Fe and Ti–Ni systems [1]. As a result of the formation of these intermetallic compounds, a σ-FeCr phase would be generated on the SUS304 side (Layer 3) as a denuded zone of Ni and Fe.

Table 2 shows the diffusion coefficients of Ti in γ-Fe and Fe and those of Cr and Ni in β-Ti at 1350 K by D_0: frequency factor and Q:

Table 1
Chemical compositions of materials used in this study (mass%).

	C	Si	Mn	P	S	Ni	Cr	H	O	N	Fe	Ti
CP-Ti	0.01	–	–	–	–	–	–	0.001	0.009	–	0.03	Bal.
SUS304	0.06	0.53	0.98	0.032	0.005	8.09	18.28	–	–	–	Bal.	–

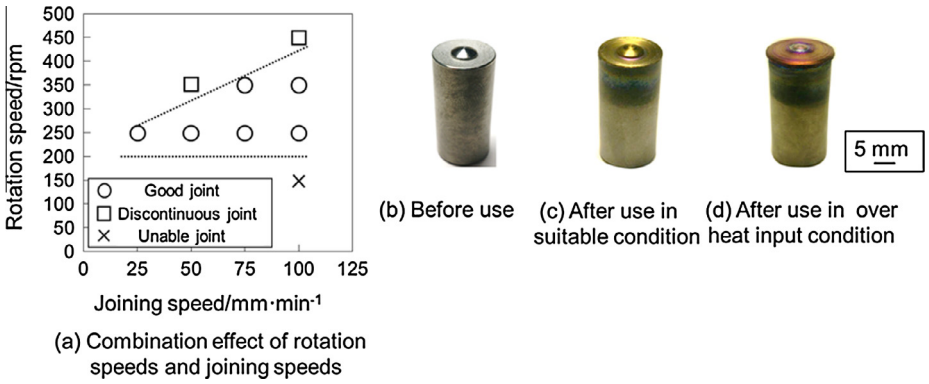

Fig. 3. (a) Combination effect of rotation speeds and joining speeds on the lap joint formation of CP-Ti/SUS304. Images of the FSW tool (b) before joining, (c) after joining at a suitable temperature, and (d) after joining with excess heat generation.

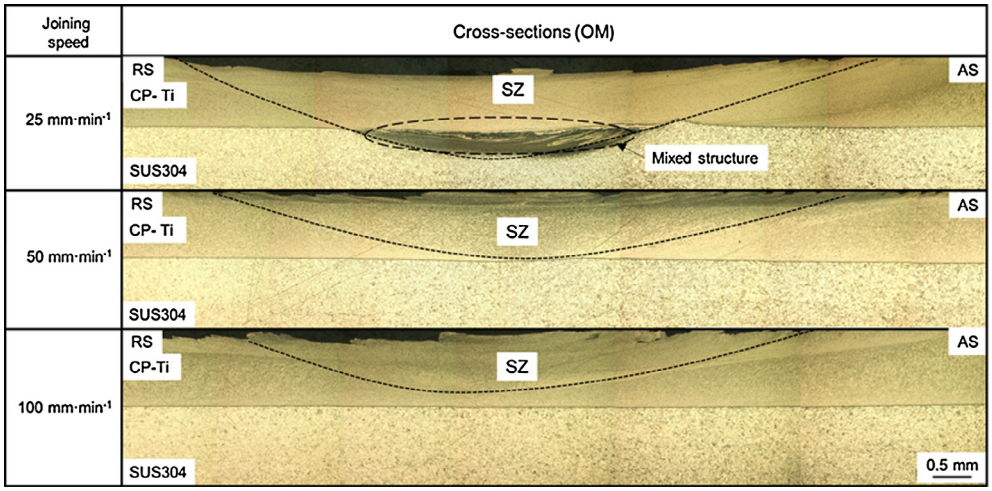

Fig. 4. Microstructures of the cross section of FSW lap joints with joining speeds of 25, 50, and 100 mm min^{-1} at a constant rotation speed of 250 rpm.

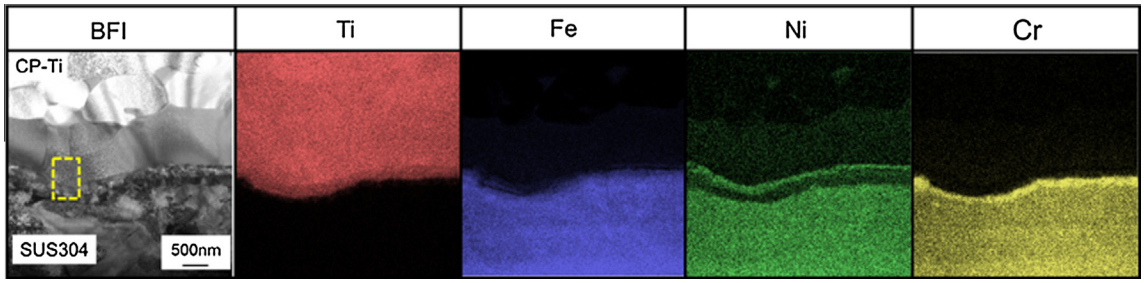

Fig. 5. TEM BFI and element distributions of Ti, Fe, Ni, and Cr at the interface of the CP-Ti/SUS304 FSW lap joint at a tool rotation speed of 250 rpm, and a joining speed of 50 mm min^{-1}.

activation energy of diffusion [Eq. (1)]. The diffusion coefficients of Fe, Cr, and Ni in β-Ti are far larger than the diffusion coefficient of Ti in γ-Fe, and the magnitude of the diffusion coefficients of these elements in β-Ti are in the order of Ni > Fe > Cr. Thus, Ni, Fe, and Cr in SUS304 preferentially diffused to the CP-Ti side during FSW. As a result, the intermetallic compound layers of Ti_2Ni, FeTi, Fe_2Ti, and σ-FeCr were generated as lamellar layers in order.

$$D = D_0 \exp\left(\frac{-Q}{RT}\right) \quad (1)$$

In this equation, R is the gas constant, 8.314 J K^{-1} mol^{-1}, and T (K) is the temperature.

Ghosh et al. [2,3] have reported the research results of diffusion bonding between commercially pure titanium and 304 stainless steel at 850 °C for 2 h. The formation of a layer of the intermetallic compounds FeTi, Fe_2Ti, and σ-FeCr has been confirmed and its thickness was about 7 μm after bonding at 850 °C for 2 h. The thickness of the intermetallic compound layer of our FSW joint was 300 nm, which is much lower than that of diffusion bonding. The FSW process needs only a short heating time compared with diffusion bonding, therefore the growth of the intermetallic compound layer would be reduced.

Fig. 7 shows the backscattered electron image (BEI) and element distributions of Ti, Fe, Ni, and Cr in the interfacial mixed

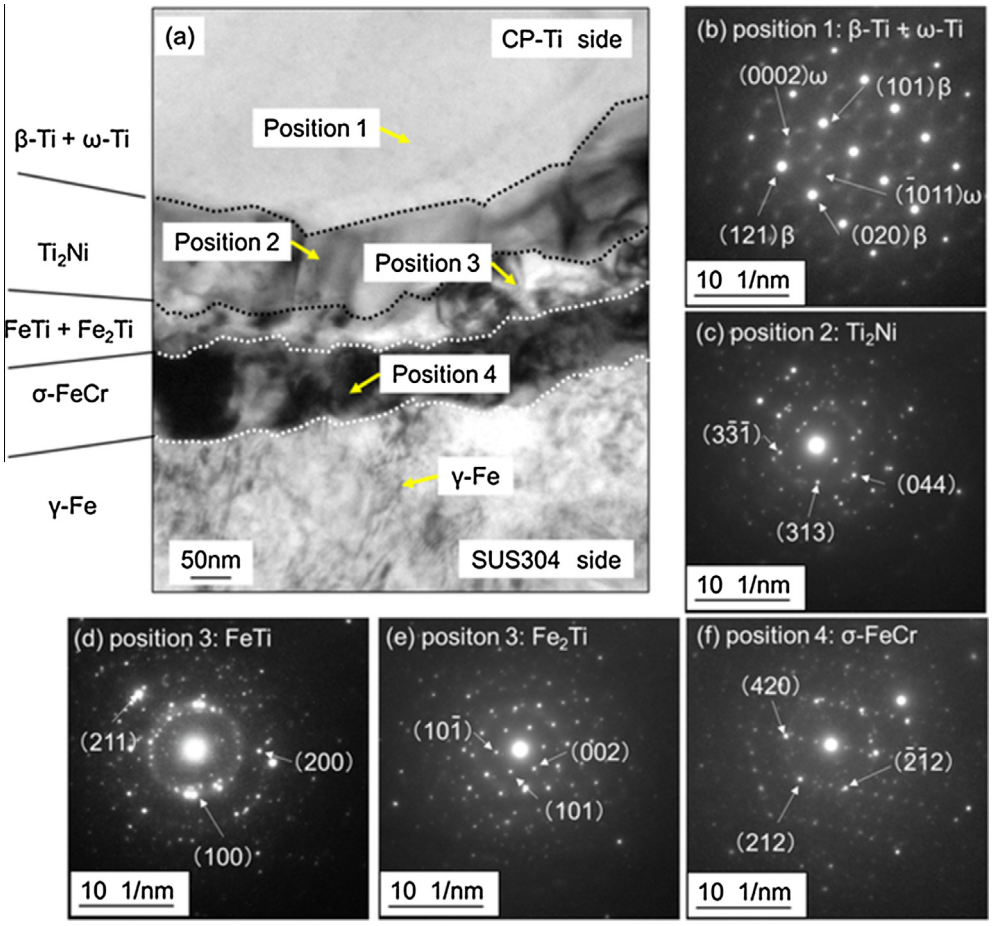

Fig. 6. TEM micrograph at the interface of the CP-Ti/SUS304 FSW lap joint at a tool rotation speed of 250 rpm, and a joining speed of 50 mm min^{-1}: (a) overview of the interface and SAD patterns of (b) β-Ti and ω-Ti phases at Position 1, (c) a Ti_2Ni phase at Position 2, (d) FeTi and (e) Fe_2Ti phases in Position 3, and (f) σ-FeCr phase in Position 4.

Table 2
Diffusion coefficients of Ti in γ-Fe and Fe, Cr, and Ni in β-Ti at 1350 K.

Matrix	Diffuse element	D (m^2 s^{-1})	D_0 (m^2 s^{-1})	Q (kJ mol^{-1})
γ-Fe	Ti	2.88E−15	1.50E−5	251
β-Ti	Fe	1.06E−11	8.00E−7	126
β-Ti	Cr	8.84E−13	7.40E−7	153
β-Ti	Ni	1.32E−11	1.70E−6	132

structure at the joint interface at a joining speed of 25 mm min^{-1} and a tool rotation speed of 250 rpm. The mixed structure consisted of laminated layers of different compositions.

Fig. 8 shows TEM micrographs of the mixed structure on the SUS304 side near the joint interface at a joining speed of 25 mm min^{-1} and a tool rotation speed of 250 rpm. The bright area corresponds to the phase with a higher Ti content (>80 mass%), which would be β-Ti and ω-Ti, whereas the dark area corresponds to phases with lower Ti content. The bright area at the bottom was originally the CP-Ti layer, which diffused into the SUS304 side.

Fig. 8b and c shows the high-magnification BFIs of the areas indicated by broken lines in Fig. 8a. Table 3 gives the measured chemical compositions and estimated phases at Positions 1–8 in Fig. 8b and c. The phases of Positions 1–8 were identified as Ti_2(Ni, Fe), FeTi and Fe_2Ti, σ-FeCr, γ-Fe, FeTi, FeTi and Fe_2Ti, σ-FeCr, and γ-Fe, respectively.

Ti_2(Ni, Fe) would be a substitutional compound of Ti_2Ni. Fe can be substituted for Ni in intermetallic compounds of Ti_2Ni according to the Fe–Ni–Ti ternary phase diagram [15].

The mixed structure formed with a joining speed of 25 mm min^{-1} consisted of the same intermetallic compounds as the flat and smooth interface formed at a joining speed of 50 mm min^{-1} shown in Fig. 5.

Since CP-Ti and SUS304 were stirred strongly by the pin at the low joining speed of 25 mm min^{-1} owing to its high heat input, which resulted in softening of the CP-Ti and an increase of the pin plunge depth, macroscopically mixed structures between CP-Ti and SUS304 were formed first. Then, the mutual diffusion of each alloying element formed a macroscopically mixed and laminated structure consisting of multiple layers of β-Ti and intermetallic compounds.

At the tensile shear test, the CP-Ti base plate of all the samples fractured at some distance from the FSW zone, regardless of joining speed, as shown in Fig. 9. Typical fractured joints are shown for the various joining speeds at a constant tool rotation speed of 250 rpm. The tensile shear strength of the joints was approximately 4.6 kN, corresponding to the strength of the CP-Ti base plate.

Fig. 10 shows the relationship between the joining speed and the peel strength of the CP-Ti/SUS304 FSW lap joint at a constant tool rotation speed of 250 rpm. Fig. 11(a) shows typical fractured joints after peel test. During the peel test, all the joints were fractured at the joint interface. The peel strength of the FSW joint increased with increasing joining speed up to 50 mm min^{-1} and then decreased at 100 mm min^{-1}. Thus, the joining speed of 50 mm min^{-1} was determined to be the optimum joining speed to obtain the strongest peel strength owing to the formation of a

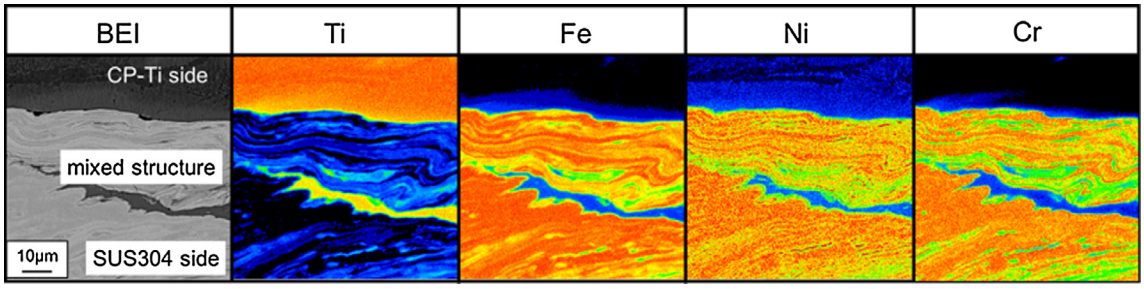

Fig. 7. BEI and element mapping of interfacial mixed region of the CP-Ti/SUS304 FSW lap joint at a tool rotation speed of 250 rpm, and a joining speed of 25 mm min^{-1}.

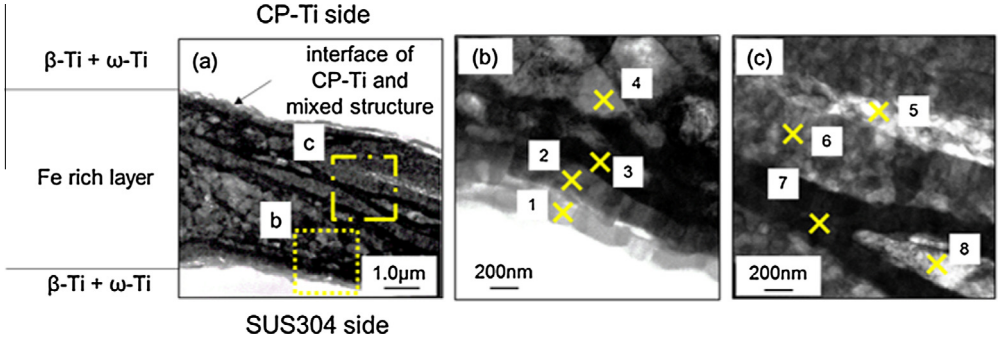

Fig. 8. (a) TEM BFI of the mixed structure at the joint interface of the CP-Ti/SUS304 FSW lap joint at a tool rotation speed of 250 rpm and a joining speed of 25 mm min^{-1}. (b and c) High-magnification images of the areas shown by the broken lines in (a).

Table 3
Element analysis results of the micro-intermixing zone and estimate phases.

Position	Element (at%)				Estimated phases
	Ti	Fe	Cr	Ni	
1	62.4	25.0	2.8	9.8	$Ti_2(Ni, Fe)$
2	32.3	54.1	9.7	3.9	$TiFe + TiFe_2$
3	12.6	60.4	23.8	3.2	σ-CrFe
4	4.6	69.7	18.7	7.0	γ-Fe
5	46.3	38.1	7.1	8.5	FeTi
6	31.2	51.8	11.5	5.5	$TiFe + TiFe_2$
7	8.7	64.0	22.0	5.3	σ-CrFe
8	3.1	70.6	19.2	7.1	γ-Fe

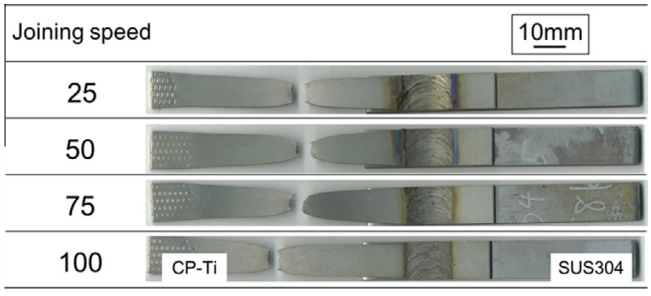

Fig. 9. Appearance of the fractured joint after tensile shear test of the CP-Ti/SUS304 FSW lap joint.

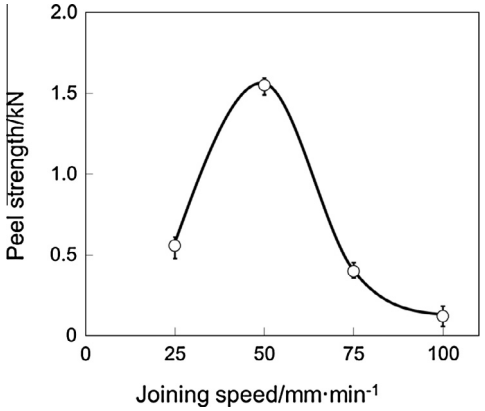

Fig. 10. Relationship between the joining speed and the peel strength.

very thin reaction layer that consisted of diffusion and intermetallic compound layers at the joint interface.

Fig. 11(b) shows SEM secondary electron images (SEI) and the elemental distribution of Ti and Fe on the fractured surface of CP-Ti and SUS304 with a joining speed of 50 mm min^{-1} after the peel test. The fractured surface was divided into two areas (Area 1 and 2 in the SEI of Fig. 11(b)). In Area 1, the fractured Ti base material was detected on the SUS304 side. In Area 2, the fracture must have mainly occurred in the intermetallic compound layer because Fe and Ti were detected on both fractured surfaces.

As the heat input per unit length of the joint decreased with increasing joining speed, the reaction layers would not be formed uniformly along the joint interface because the stirring effect of the pin would be weakened. As a result, the joint strength decreased with increasing joining speed from 50 to 100 mm min^{-1} and the peel strength decreased with decreasing joining speed from 50 to 25 mm min^{-1}. The joint formed with a joining speed of 25 mm min^{-1} had the mixed structure. The mixed structure consisted of laminates of intermetallic compounds and the thickness of the joint interface was as much as 300 μm. Therefore, the peel strength of the FSW joint decreased with decreasing joining speed.

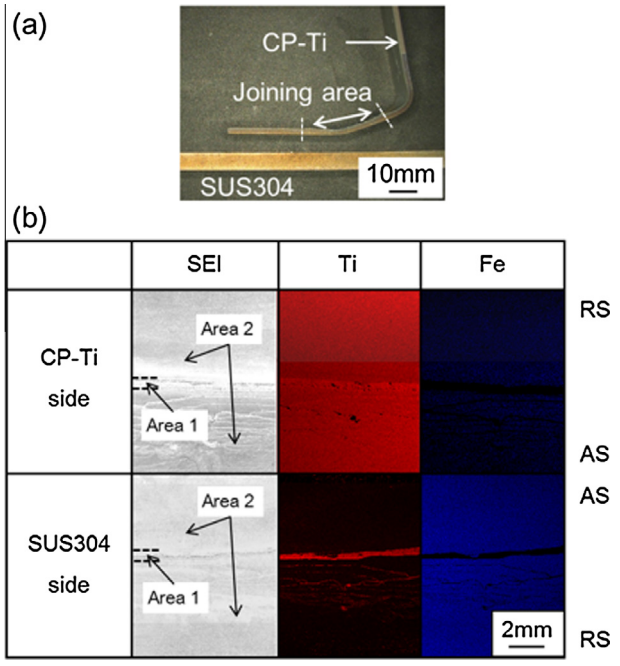

Fig. 11. (a) Appearance of the typical fractured joint after peel test of the CP-Ti/SUS304 FSW lap joint. (b) SEI and element distributions on the fractured surface of CP-Ti and SUS304 after peel test at a joining speed 50 mm min^{-1}.

4. Conclusion

Friction stir welding was perform to accomplish the dissimilar-lap joining of CP-Ti/SUS304. At a constant tool down-force of 9.8 kN and tool rotation speed of 250 rpm, the joining speed was varied from 25 to 100 mm min^{-1} to investigate the effect of the joining speed on the interface structure, tensile shear strength, and peel test strength of the joint. We arrived at the following conclusions:

(1) The cross section of the joint with a joining speed 50 mm min^{-1} showed a flat and smooth interface with no voids or cracks. Reaction layers consisting of β-Ti (+ ω-Ti), Ti_2Ni, FeTi + Fe_2Ti, and σ-FeCr, arranged in order from the CP-Ti side to the SUS304 side, were formed along the interface. The total thickness of the reaction layer was approximately 1 μm.

(2) At a joining speed of 25 mm min^{-1}, a macroscopically mixed and laminated structure which consisted of comparably thick β-Ti (+ ω-Ti), Ti_2Ni, FeTi + Fe_2Ti, and σ-FeCr layers.

(3) The tensile shear strength of the joint was approximately 4.6 kN for a specimen width of 12 mm, and fractures occurred in the CP-Ti base material for every joining speed.

(4) During the peel test, all the joints were fractured at the joint interface. A maximum peel strength of 1.5 kN was obtained at a joining speed of 50 mm min^{-1}; the peel strength decreased at lower or higher joining speeds than this.

References

[1] T.B. Massalski, H. Okamoto, P.R. Subramanian, L. Kacprzak, Binary Alloy Phase Diagrams, second ed., ASM International, Mater. Park, 1990. CD-ROM.
[2] M. Ghosh, K. Bhanumurthy, G.B. Kale, J. Krishnan, S. Chatterjee, Diffusion bonding of titanium to 304 stainless steel, J. Nucl. Mater. 322 (2003) 235–241.
[3] M. Ghosh, S. Chatterjee, Effect of interface microstructure on the bond strength of the diffusion welded joints between titanium and stainless steel, Mater. Charact. 54 (2005) 327–337.
[4] S.A.A. Akbari Mousavi, S.P. Farhadi, Effect of post-weld heat treatment on the interface microstructure of explosively welded titanium–stainless steel composite, Mater. Sci. Eng. A 494 (2008) 329–336.
[5] S.A.A. Akbari Mousavi, S.P. Frarhadi, Experimental investigation of explosive welding of co-titanium/AISI 304 stainless steel, Mater. Des. 30 (2009) 459–468.
[6] M. Yadegari, A.R. Ebrahimi, A. Karami, Effect of heat treatment on interface microstructure and bond strength in explosively welded Ti/304L stainless steel clad, Mater. Sci. Technol. 29 (2013) 69–75.
[7] T. Wang, B.G. Zhang, G.Q. Chen, J.C. Feng, Q. Tang, Electron beam welding of Ti-15-3 titanium alloy to 304 stainless with copper interlayer sheet, Trans. Nonferr. Mater. Sci. China 20 (2010) 1829–1834.
[8] M.F. Najafabadi, S.F.K. Bozorg, A.Z. Hanzaki, Joining of CP-Ti to 304 stainless steel using friction stir welding technique, Mater. Des. 31 (2010) 4800–4807.
[9] M.F. Najafabadi, S.F.K. Bozorg, A.Z. Hanzaki, Dissimilar lap joining of 304 stainless steel to CP-Ti employing friction stir welding, Mater. Des. 32 (2011) 1824–1832.
[10] J. Liao, N. Yamamoto, H. Liu, K. Nakata, Microstructure at friction stir lap joint interface of pure titanium and steel, Mater. Lett. 64 (2010) 2317–2320.
[11] H.Y. Kim, Y. Ikehara, J.I. Kim, H. Hosoda, S. Miyazaki, Martensitic transformation, shape memory effect and superelasticity of Ti–Nb binary alloys, Acta Mater. 54 (2006) 2419–2429.
[12] M. Todai, T. Fukuda, T. Kakeshita, Relation between negative temperature coefficient in electrical resistivity and a thermal ω phase in Ti–xNb ($26 \leqslant x \leqslant 29$ at.%) alloys, J. Alloys Comp. 577 (2013) 431–434.
[13] J. Liao, N. Yamamoto, K. Nakata, Effect of intermetallic compound layer on tensile strength of dissimilar friction-stir weld of a High Strength Mg Alloy and Al Alloy, Mater. Trans. 40A (2009) 2212–2219.
[14] A. Kostka, R.S. Coelho, J. Dos Santos, A.R. Pyzalla, Microstructure of friction stir welding of aluminium alloy to magnesium alloy, Scr. Mater. 60 (2009) 953–956.
[15] L.I. Duarte, U.E. Klotz, C. Leinenbach, M. Palm, F. Steinc, J.F. Loffler, Experimental study of the Fe–Ni–Ti system, Intermetallics 18 (2010) 374–384.